Dielectric Relaxation Studies of 4-*n*-Alkyloxy-4′-Cyanobiphenyls (*n*OCB, $n = 5 \div 8$)

S. Urban[a], B. Gestblom[b], H. Kresse[c], and R. Dąbrowski[d]

[a] Institute of Physics, Jagellonian University, Reymonta 4, 30-059 Cracow, Poland
[b] Institute of Physics, Uppsala University, Uppsala, Sweden
[c] Institute of Physical Chemistry, Martin-Luther-University, Halle, Germany
[d] Institute of Chemistry, Military Technical Academy, Warsaw, Poland

Z. Naturforsch. **51a,** 834–842 (1996); received February 17, 1996

The results of dielectric relaxation studies of series of four *n*-alkyloxy cyanobiphenyl (*n*OCB) compounds with *n* ranging from 5 to 8 are presented. The complex dielectric permittivity, $\varepsilon^*(\omega) = \varepsilon'(\omega) - i\,\varepsilon''(\omega)$, was measured in the frequency range 1 kHz–3 GHz, with the use of an impedance analyzer and a time domain spectroscopy (TDS) set-up. The relaxation times: longitudinal $\tau_{\|}$ in the nematic and smectic A phase (8 OCB), transverse $\tau_{\perp}$ in the nematic phase, and τ_{is} in the isotropic phase, were obtained as functions of the temperature. This allowed the calculation of activation barriers for different molecular relaxation processes occurring in particular phases. Moreover, the retardation factors $g_{\|}$ and $g_{\perp}$ and the nematic potential q according to two theoretical models were calculated. The analysis of $q(T)$ and its relation to the order parameter S is done taking into account the results of NMR studies of the compounds under consideration. Finally, the dependencies of the obtained quantities on the number of carbon atoms in the alkyloxy chains are analyzed.

Introduction

The properties of liquid crystalline (LC) phases can be studied by the dielectric method. Static permittivity measurements give information about the dielectric anisotropy, $\Delta\varepsilon = \varepsilon_{\|} - \varepsilon_{\perp}$, of a LC phase in relation to the dipole moment of a molecule, while measurements of the dielectric dispersion, $\varepsilon'(\omega)$, and absorption, $\varepsilon''(\omega)$, enables one to study different relaxation processes associated with the anisotropic reorientation of the dipolar molecules in LC phases. Two main types of reorientations, those around the short (low frequency, l.f., process) and around the long molecular axes (high frequency, h.f., process), occur with different time scales. Additionally, both these motions can be easily distinguished by a proper orientation of the director ***n*** in relation to the probing electric field (parallel, $\boldsymbol{E} \parallel \boldsymbol{n}$, and perpendicular, $\boldsymbol{E} \perp \boldsymbol{n}$, respectively). In the isotropic phase these relaxation processes merge, giving one broad spectrum. Since several experimental techniques must be used for seeing particular processes, comprehensive dielectric studies of LCs are rather scarce. In this paper we report on dielectric investigations of four *n*-alkyloxy-cyanobiphenyls (*n*OCB, $n = 5$, 6, 7, 8), carried out with two separate equipments for impedance measurements in the frequency range 1 kHz–13 MHz and time domain spectroscopy (TDS) [1] in the frequency range 10 MHz–5 GHz.

The substances belonging to the *n*OCB homologous series are used for the preparation of LC mixtures applied in the display technology. The members with $n \leq 7$ form the nematic phase whereas those with $n \geq 8$ exhibit also (or exclusively) the smectic A_d polymorphism [2]. 8 OCB is known to show the reentrant phenomenon under high pressure [3, 4]. The *n*OCB molecules possess a large longitudinal dipole moment caused by the strongly polar terminal CN group; this gives a pronounced relaxation spectrum in the MHz frequency range at $\boldsymbol{E} \parallel \boldsymbol{n}$ geometry (the l.f. process). However, due to the alkyloxy group placed at the opposite side of the biphenyl core, also a small perpendicular component of the dipole moment is present that can give some contribution to the high frequency relaxation process observed in the GHz frequency range at $\boldsymbol{E} \perp \boldsymbol{n}$ geometry. In spite of their potentially interesting dielectric properties, the *n*OCB compounds, except 7 OCB [5], have not been studied over a wide frequency range [6, 7]. In contrast, they have been intensively investigated with the use of deuterium NMR techniques [8–11]. Some aspects of these studies can be useful for the discussion of the dielectric results.

Reprint requests to Prof. S. Urban.

0932-0784 / 96 / 0700-0834 $ 06.00 © – Verlag der Zeitschrift für Naturforschung, D-72072 Tübingen

The molecular dynamics in LC phases is governed by the nematic or smectic potential (q) which arises from the strongly anisotropic interactions between rod-like molecules. In the Maier and Saupe mean-field theory of the nematic state [12] it was supposed that the orientation dependent potential energy of one molecule in the field of its neighbors is given in the form

$$U(\theta) = -q P_2(\cos\theta), \tag{1}$$

where $P_2(\cos\theta)$ is the second rank Legendre polynomial. It was assumed that the nematic potential is proportional to the order parameter $S = \langle P_2(\cos\theta)\rangle$,

$$q = \mathscr{E} S, \tag{2}$$

where the interaction coefficient $\mathscr{E}$ determines the energy scale of the potential and is temperature independent. Theoretical considerations predict that this potential hinders strongly the reorientations of molecules around the short axes, whereas the reorientation around the long axis is even facilitated in relation to the motion in the isotropic liquid [13–19]. In order to consider quantitatively the effect of the nematic potential on molecular reorientations, Meier and Saupe [13] have introduced the so-called retardation factors defined as $g_\parallel = \tau_\parallel/\tau_0 (> 1)$ and $g_\perp = \tau_\perp/\tau_0 (< 1)$, where τ_0 corresponds to the situation when $q = 0$; in practice, τ_0 is estimated by extrapolation of τ_{is} to the nematic phase [13, 20–22]. There are two expressions relating the parallel retardation factor $g_\parallel$ with the nematic potential q. Originally Meier and Saupe [13] considered the l.f. relaxation process in the Maier-Saupe potential assuming that the perturbation of the angular distribution function by the probe electric field has the form of a cosine at all times after the field is switched off. In this manner they circumvented the need for solving the equation for the distribution function exactly. They obtained the relation

$$g_\parallel = \frac{\tau_\parallel}{\tau_0} = \frac{e^\sigma - 1}{\sigma} \tag{3}$$

with the nematic potential barrier parameter $\sigma = q/RT$.

Recently Coffey et al. [16–19] have developed a new approach to the problem of Brownian rotational motions of a single axis rotator in a uniaxial potential. Using very sophisticated mathematical procedures, the authors have obtained the exact analytic solution for the retardation factors $g_\parallel$ and $g_\perp$ in terms of σ. The following formula for the parallel retardation factor approximates closely the exact solution for all σ:

$$g_\parallel = \frac{\tau_\parallel}{\tau_0} = \frac{e^\sigma - 1}{\sigma}\left(\frac{2}{1 + 1/\sigma}\sqrt{\sigma/\pi} + 2^{-\sigma}\right)^{-1}. \tag{4}$$

The two formulae differ considerably, especially for $\sigma > 1$. Therefore the q values calculated with (4) are approximately 25% greater than those obtained with (3), see [23, 24]. Coffey et al. [16, 19] give also the relations between the retardation factors $g_\parallel$ and $g_\perp$ and the order parameter S:

$$g_\parallel^S = \frac{2S + 1}{1 - S}, \quad g_\perp^S = \frac{2 - 2S}{2 + S}. \tag{5}$$

However, the expression for the longitudinal retardation factor does not provide a correct description of the behavior of $g_\parallel$ for $\sigma > 2$, whereas the one for $g_\perp$ is valid for all σ [18, 19]. By combination of the Eqs. (5) one gets the general relationship between the retardation factors

$$(g_\parallel + 1) g_\perp = 2. \tag{6}$$

A discussion of the relationships (3)–(6) is given in [23, 24]. The present results can also be discussed in terms of the above relations.

Experimental

The *n*OCB samples were produced by one of us (R. D.). Their transition temperatures are listed in Table 1. They agree very well with the literature data [2].

The measurements of $\varepsilon_\parallel^*(f) = \varepsilon_\parallel'(f) - i\varepsilon_\parallel''(f)$ for the nematic phase of 5OCB, 6OCB and 7OCB, and for the smectic phase of 8OCB were performed in the frequency range of 1 kHz–13 MHz using a HP 4192 A impedance analyzer. A parellel-plate capacitor ($A \approx 1$ cm^2) was calibrated with the use of standard liquids. The distance between electrodes was 0.2 mm. The samples were oriented by both the electric DC ($E \approx 1500$ V/cm) and magnetic ($B \approx 0.7$ T) fields.

Table 1. Transition temperatures (in °C) for *n*OCB compounds.

Substance	5OCB	6OCB	7OCB	8OCB
Melting	48.0	57.0	54.0	54.5
Smectic A–nematic	–	–	–	67.5
Nematic–isotropic	68.0	75.5	74.0	80.5

Starting from the isotropic liquid, the samples were slowly cooled down step by step. This allowed considerable supercooling of the samples below the nominal freezing points. The temperature was stabilized within ± 0.1 K.

The measurements of $\varepsilon_{\mathrm{is}}^*$ in the isotropic phase and $\varepsilon_\perp^*$ in the nematic phase of all four substances, and $\varepsilon_\parallel^*$ in the nematic phase of 8 OCB, were performed with the aid of the time domain spectroscopy technique (TDS). The experimental details can be found in [1, 23, 24]. In the case of the isotropic phase, two time windows were used (10 ns and 100 ns) and then the spectra were spliced as described in [24]. For the nematic phase of 8 OCB, the 200 ns time window was used, which allowed for covering the frequency range from ca. 2 MHz to ca. 400 MHz. In this case the orientation of the sample was not perfect, however, and therefore the static permittivities (extrapolated) are markedly lower than those obtained in other studies [6, 7]; it was proved [25] that this fact does not alter the values of the relaxation times determined from the position of $\varepsilon''_{\mathrm{max}}$. The spectra for $\boldsymbol{E} \perp \boldsymbol{n}$ geometry were collected in the same way as in the isotropic phase.

Results

The dielectric spectra in the form of Cole-Cole plots ε'' vs. ε', measured in different phases of partcicular substances, are shown in Fig. 1 (the LC phases) and Fig. 2 (the isotropic phase). The particular spectra were analyzed with the well known Debye, Cole-Cole (C-C) and Davidson-Cole (D-C) equations [26]

$$\text{(C-C)}\ \frac{\varepsilon^* - \varepsilon_\infty}{\varepsilon_s - \varepsilon_\infty} = \frac{1}{1 + (i\,\omega\,\tau_0)^{1-\alpha}}\,;$$

$$\text{(D-C)}\ \frac{\varepsilon^* - \varepsilon_\infty}{\varepsilon_s - \varepsilon_\infty} = \frac{1}{1 + (i\,\omega\,\tau_0)^{\beta}}\,, \qquad (7)$$

where ε_s and ε_∞ are the static and high frequency permittivities, respectively, and α and β characterize the distributions of the relaxation times (symmetric and non-symmetric, respectively).

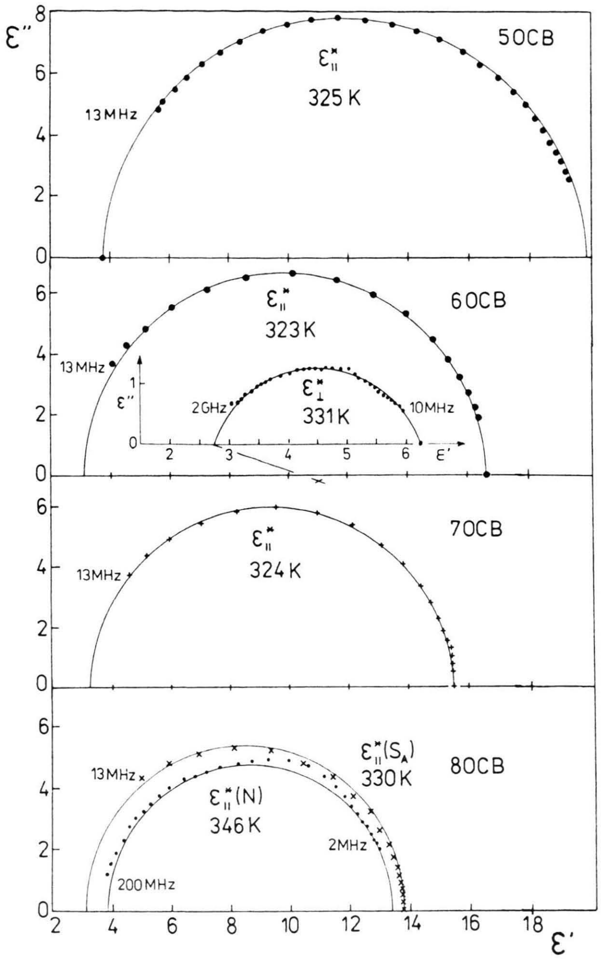

Fig. 1. Cole-Cole plots for LC phases of four *n*OCB compounds. In case of $\varepsilon_\parallel^*(\omega)$ spectra, the lines correspond to the Debye equation. One typical spectrum obtained at $\boldsymbol{E} \perp \boldsymbol{n}$ geometry is shown for the nematic phase of 6 OCB, which can be described by the Cole-Cole equation with $\alpha \approx 0.25$.

In the case of $\boldsymbol{E} \parallel \boldsymbol{n}$ geometry (nematic and smectic phases) we are dealing with a single relaxation process well described by the Debye equation ($\alpha = 0$) with the relaxation time $\tau_\parallel$ as the fitting parameter (see Figure 1). The obtained relaxation times are shown in Figure 3. In order to avoid the temperature shifts they are presented as $\log \tau$ versus $(1/T - 1/T_{\mathrm{NI}})$, which is equivalent to Arrhenius plots. The calculated activation enthalpies $\Delta H_\parallel$ are listed in Table 2.

Concerning the h.f. relaxation process appearing at the $\boldsymbol{E} \perp \boldsymbol{n}$ geometry, the quality of the TDS spectra was rather poor due to weak intensity of the dielectric loss $\varepsilon''_\perp$. A typical spectrum obtained for 6 OCB is shown in Fig. 1 (in fact there are two spliced spectra). The shapes of the $\varepsilon_\perp^*(\omega)$ spectra suggest that they consist of different relaxation processes which cannot be easily separated. Therefore the spectra were analyzed with the use of the Cole-Cole equation with a large parameter characterizing the distribution of the relaxaion times ($\alpha \sim 0.25$). The calculated relaxation

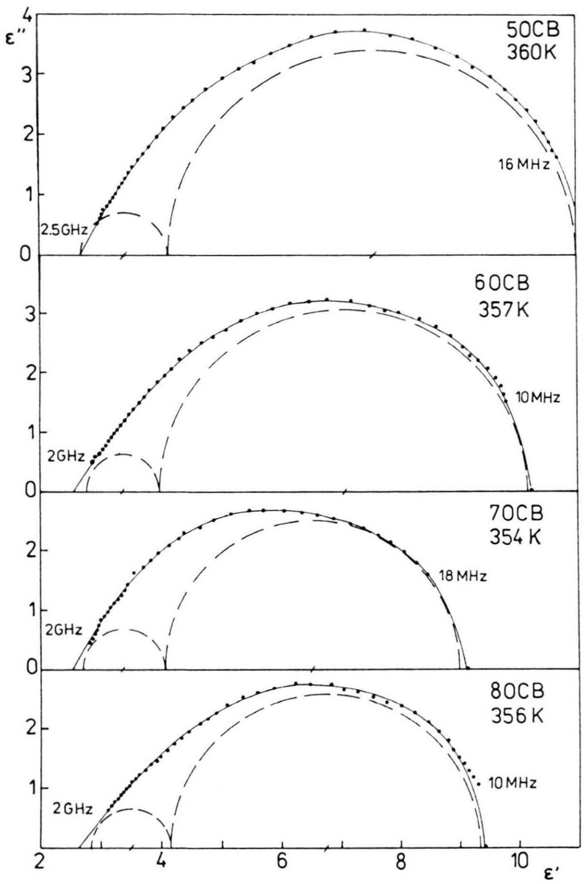

Fig. 2. Cole-Cole plots for the isotropic phase of *n*OCB compounds. The solid lines correspond to the Davidson-Cole equation. The dashed semicircles illustrate a possible division of the spectrum into two Debye-type relaxation processes.

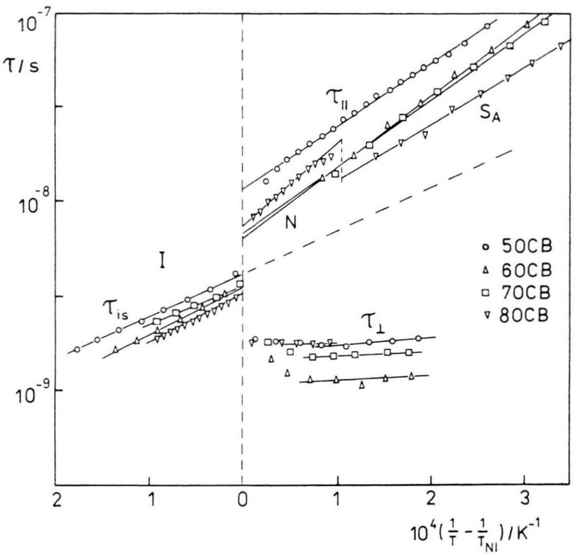

Fig. 3. Log τ vs. $(1/T - 1/T_{NI})$ for different relaxation processes shown in Figures 1 and 2. A non-typical unit in the abscissa was taken in order to avoid the shifts caused by different nematic-isotropic transition temperatures of the substances. The dashed line shows the extrapolation of the relaxation time τ_{is} to the nematic phase.

Table 2. The parameters of the Arrhenius equation $\tau = A \cdot \exp(\Delta H/RT)$ obtained for different phases of *n*OCB compounds.

Substance	Phase	A/sec	ΔH/kJ mol^{-1}
5OCB	isotropic	9.54×10^{-16}	43.3 ± 1
	nematic ∥	1.89×10^{-19}	70.0 ± 1
	nematic ⊥	2.77×10^{-10}	5.1 ± 1
6OCB	isotropic	6.48×10^{-15}	37.9 ± 1
	nematic ∥	4.36×10^{-19}	68.2 ± 1
	nematic ⊥	1.16×10^{-16}	6.4 ± 1
7OCB	isotropic	4.65×10^{-15}	39.1 ± 1
			49 ± 5 [5]
	nematic ∥	1.41×10^{-18}	64.6 ± 1
			65 ± 5 [5]
	nematic ⊥	3.30×10^{-10}	4.2 ± 1
			<4 [5]
8OCB	isotropic	1.32×10^{-16}	50.0 ± 1
	nematic ∥	7.16×10^{-20}	74.6 ± 2
	nematic ⊥	–	<3
	smectic A_d ∥	3.28×10^{-17}	56.2 ± 1

times $\tau_{\perp}$ are shown in Fig. 3, and the activation parameters are presented in Table 2.

The TDS spectra of the isotropic phase are deformed at the high frequency wing. One can suppose (see discussion) that they consist of two relaxation processes with considerably different amplitudes and relaxation times. Therefore we tried to fit to them two Debye-type semicircles (dashed curves in Figure 2). Unfortunately, due to a large difference in the amplitudes of both contributions, the analysis of the spectra measured at different temperatures did not give a consistent separation. The best fits were obtained when the Davidson-Cole equation was used (solid lines). Additionally, the frequencies f_c corresponding to the maximum of losses ε''_{max} were calculated. In fact, all calculated relaxation times τ_{is} characterizing the main relaxation process in the isotropic phase were very close for all models, similarly to the case of 7 PCH [24]. The average values of τ_{is} are shown in Fig. 3, and the parameters of the Arrhenius equation are listed in Table 2.

Discussion

The molecules of *n*OCB compounds possess two dipole groups: the cyano-CN group gives a strong component along the main molecular axis, and the alkyloxy $H_{2n+1}C_nO$-group gives a dipole moment deflected by ca. 72° from that axis. Due to this, both the longitudinal, μ_l, and the transverse, μ_t, components of the dipole moment may give contributions to the relaxation spectra in LC phases as well as in the isotropic phase. The group dipole moment calculations [27] yield $\mu_l = 4.40$ D and $\mu_t = 1.22$ D, with the resultant dipole moment of 4.57 D. Because the dielectric increment $\delta\varepsilon = \varepsilon_s - \varepsilon_\infty$ is roughly proportional to μ^2, the relaxation process governed by the longitudinal component should dominate over the transverse one in the substances under consideration. According to the mean-field theory [4, 12, 20, 21] the relative intensities of the absorptions given by both components of the dipole moments in the nematic phase are: $\mu_l^2(1+2S)/\mu_t^2(1-S)$ for the $\boldsymbol{E} \parallel \boldsymbol{n}$ geometry, and $\mu_l^2(1-S)/\mu_t^2(1+S/2)$ for the $\boldsymbol{E} \perp \boldsymbol{n}$ geometry, which (assuming $S = 0.6$) leads to ca. 70:1 and 4:1 for the ratios of amplitudes at the two geometries, respectively, whereas for the isotropic phase the ratio is ca. 13:1. This shows that a real influence of both main molecular reorientations on the $\varepsilon_\perp^*(\omega)$ and $\varepsilon_{is}^*(\omega)$ relaxation spectra of the *n*OCB compounds can be expected. This is well seen in Figs. 1 and 2. In the spectra of the isotropic phase (Fig. 2) the h.f. process appears as a small wing at GHz frequencies (see also Buka et al. [5]). The l.f. process in the N and S_A phases is a monodispersive one, while the spectra measured at the perpendicular geometry are broad. Probably they consist of at least two processes, i.e. the molecular rotations around the long axes and a small angle fluctuation of the dipole moment in respect to the director, which are characterized by similar relaxation times. This causes that they cannot be separated and only the mean relaxation time $\tau_\perp$, presented in Fig. 3, could be calculated.

The activation enthalpies, calculated from the data of Fig. 3, are presented in Table 2. In the isotropic phase the highest values of $\Delta H_{is} = 50$ kJ/mol is observed for 8OCB that is markedly larger than $\Delta H_\eta = 30$ kJ/mol obtained from the viscosity measurements [28]. Such difference may arise in part from the fact that the cyanobiphenyl molecules form antiparallel dimers even in the isotropic phase [5] and the association energy contributes to the activation enthalpy. Also the enthalpy $\Delta H_\parallel$ is highest for 8OCB. It should be mentioned, however, that 8OCB has the smectic A phase and a relatively narrow range of the nematic phase. In such situation the nematic phase may show some peculiar properties [21]. Therefore the present measurements were performed in steps of ca. 1 K in both the nematic and isotropic phase of 8OCB. It is characteristic that the activation barrier hindering molecular reorientations around the short axes in the S_A phase is distinctly lower than the corresponding barrier in the N phase, similarly to many other substances exhibiting the $N-S_A$ polymorphism [29, 30]. Dielectric studies of 8CB [31] and 8OCB [32] under high pressure have shown that the pressure influences the activation enthalpies in the N and S_A phases of these compounds, but marked differences between the activation enthalpies of both phases persist up to ca. 100 MPa. It should be added that a considerable decrease of $\Delta H_\parallel$ was also observed in the pressure studies of 5CCH when the nematic–smectic B (monotropic) transition was passed [33]. Thus it seems that the more ordered orthogonal smectic phases facilitate the molecular reorientations around the short axes.

In the case of $\boldsymbol{E} \perp \boldsymbol{n}$ geometry the relaxation times $\tau_\perp$ are distinctly shorter than the other ones and show a weak dependence on the temperature, compare Fig. 3 (the observed increase of $\tau_\perp$ in the vicinity of the clearing point is caused by a fail of orientation of the samples). Thus the molecular reorientations around the long axes are really very easy and fast, which proves a common assumption about rod-like shape or cylindrical symmetry of molecules.

The relaxation times obtained for the nematic and isotropic phase can serve for calculating the retardation factors and the nematic potential according to the formulae mentioned in the Introduction. In order to do that, the values of the order parameter S have to be known. In the literature one can find very few experimental data on $S(T)$ for the substances under study [8–11, 34]. We shall consider here the data obtained by the nuclear magnetic resonance (NMR) methods. Emsley et al. [9] have performed deuterium NMR studies of *p*-xylene-d_{10} dissolved in a series of *n*OCB compounds ($n = 1 \div 12$). The principal component S_{zz} of the second rank orientational ordering matrix can be used for our purpose. However, due to the indirect way of obtaining them, the S_{zz}-value cannot properly characterize the host-molecules' degree of orientation in the nematic phase; they are distinctly

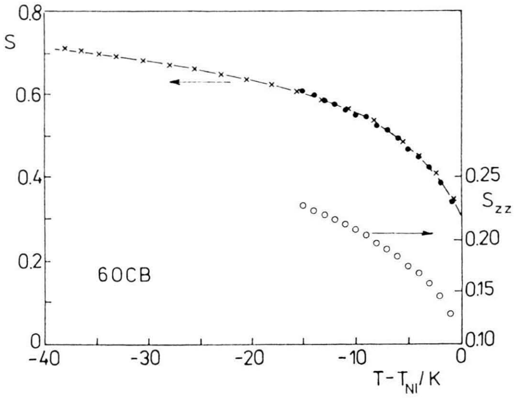

Fig. 4. Order parameter as a function of the reduced temperature ($T-T_{NI}$) in the nematic phase of 6OCB: right hand scale and open points: S_{zz} measured for *p*-xylene dissolved in the substance [9], left hand scale and crosses: S measured for a neat substance [10], full points: $2.61 \times S_{zz}$.

lower than the proper S-values. Similarly to recent studies on 7PCH [24] we asume proportionality between both quantities: $S = k S_{zz}$. In the case of 6OCB this assumption can be checked taking the $S(T)$-values obtained by Dong and Ravindranath [10], who performed NMR studies for a neat substance. Figure 4 shows both sets of S-values, those obtained by Dong et al. (×) and that calculated from Emsley et al. S_{zz}-data multiplied by the factor $k = 2.61$ (●) (these and other NMR data were taken from original figures with the aid of a computer assisted scanner). One can see a nice consistency of the experimental and normalized order parameters. Thus it seems justifiable to take the same k-factor for the calculation of S-data from the S_{zz} ones for all substances under study. They are shown in Fig. 6 as solid lines. These order parameters will be used for further discussion (this is named E + D normalization).

Another normalization can be considered if the S-data measured by Poon et al. [11] for all four *n*OCBs at $T - T_{NI} = 10$ K are taken into account. In that case a separate normalization factor for each compound has to be taken: $k = 2.31$, 2.34, 2.93 and 2.45 for $n = 5$, 6, 7 and 8, respectively. They are shown in Fig. 6 as dashed lines (named E + P normalization).

Figure 5 presents the retardation factors $g_{\parallel}$ and $g_{\perp}$ obtained for 5OCB, 6OCB and 7OCB from the data of Fig. 3 (τ_0-values were calculated by extrapolation of τ_{is} to the nematic phase as is shown in Figure 3). They

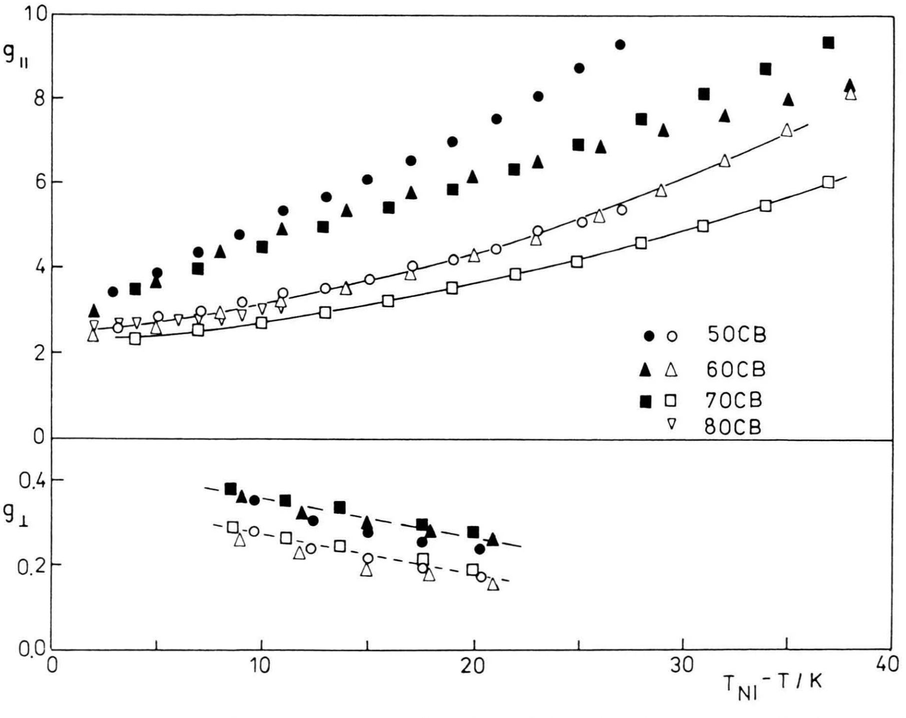

Fig. 5. The retardation factors $g_{\parallel}$ and $g_{\perp}$ as functions of the reduced temperature for the nematic phase of 5OCB, 6OCB and 7OCB. Open symbols: experimental, full symbols: calculated according to (5).

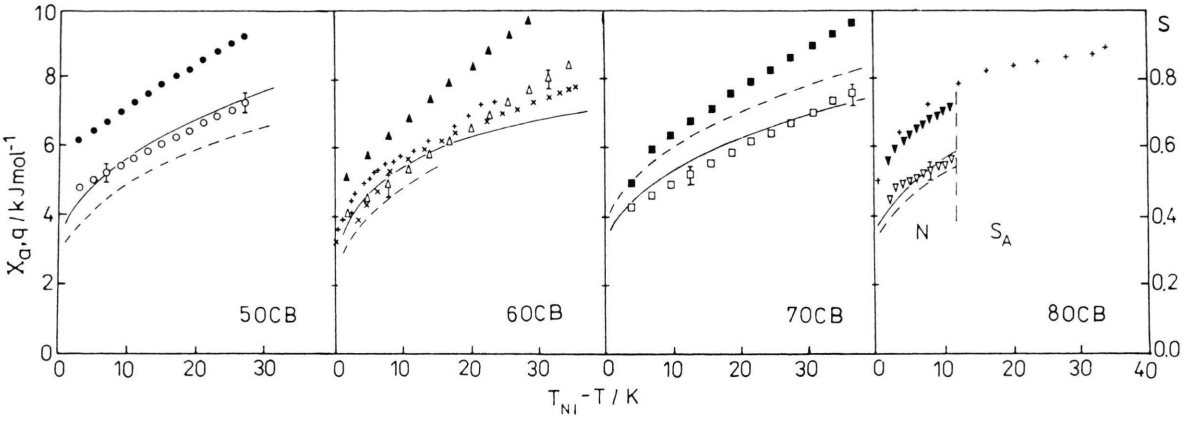

Fig. 6. The nematic potentials q and the core interaction parameter X_a (left hand scale) and the order parameter S (right hand scale) as functions of the reduced temperature for *n*OCB compounds. The open symbols correspond to Meier-Saupe (3) and full symbols to Coffey et al. (4). Solid lines are the order parameters obtained with the E + D normalization, and dashed lines with the E + P normalization (see text). X_a-data come from NMR studies of Counsell et al. [8] (+) and Dong et al. (×).

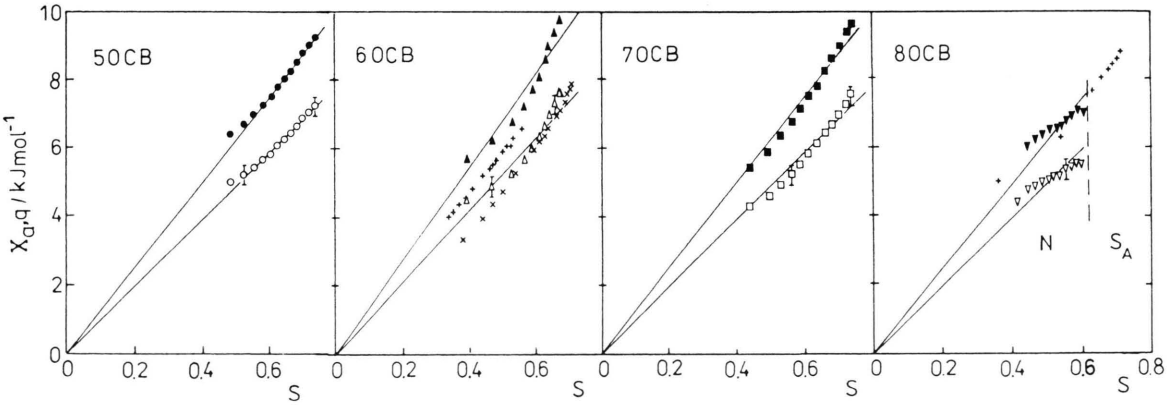

Fig. 7. q and X_a versus S plots for the nematic phase of *n*OCB compounds. The symbols have the same meanings as in Figure 6.

are compared with $g^S_{\|,\perp}$ calculated using Coffey et al. formulae (5). Large disagreement between experimental and theoretical retardation factors is observed for all substances. Moreover, the factor $(g_\| + 1) g_\perp$ is less than unity, in contradiction to the prediction of (6). (The use of S according to the E + P normalization leads to similar relations.)

For each substance the nematic potentials q were calculated according to (3) and (4). Figure 6 presents q-data versus the reduced temperature $T - T_{NI}$. One can see that the points corresponding to the Coffey et al. formula (4) (full symbols) are distinctly higher than those corresponding to the Meier-Saupe formula (3) (open symboles). They are compared with the core interaction parameter X_a obtained by Counsell et al. [8] (6OCB and 8OCB-+) and Dong et al. [10] (6OCB-×) from fitting of the theoretical order parameters to the experimental ones. In fact, the X_a parameter plays the same role in the mean-field theory considered by these authors as the nematic potential q does in the Maier and Saupe theory. As can be seen in Fig. 6, in case of 6OCB the nematic potential values obtained from the dielectric relaxation studies with the simpler Meier-Saupe formula (3) are much better consistent with both sets of NMR data than those yielded by the Coffey et al. formula (4). This concerns the values as well as the temperature dependence of q. In case of 8OCB one can observe the opposite behavior – formula (4) leads to a better agreement between the dielectric and NMR data. It should be mentioned, however, that in this substance the X_a-values were obtained in a different way than for other substances studied [8]. Counsell et al. have found a common temperature dependence of X_a for the compounds with $n = 3$, 4 and 6, and markedly different behavior for $n = 8$.

By comparison the data in Table 2 and Fig. 6 it should be noted that for all *n*OCB compounds the nematic potential does not exceed ca. 15% of the activation barrier hindering molecular rotation around the short axes. The same proportions have been found for other LC substances [23, 24, 31, 32, 35]. This indicates that the main hindrance for such rotation is caused by two other factors: friction of the medium and dipole-dipole associations between strongly polar molecules. A broader discussion of this problem can be found in [35, 36].

Table 3. Mean-field interaction coefficient $\mathscr{E}$ determined from the deuterium NMR spectra and the dielectric relaxation studies for LC substances belonging to three homologous series: *n*OCB, *n*CB and *n*PCH having strongly polar CN groups.

Substance	Interaction Coefficient $\mathscr{E}$/kJ mol^{-1}			
	NMR		Dielectric Relaxation	
			E + D norm.	E + P norm.
3 OCB	11.73	[8]		
4 OCB	11.73	[8]		
5 OCB	–		9.8 ± 0.2 [a] (12.4 ± 0.2) [b]	11.4 ± 0.2 (14.6 ± 0.2)
6 OCB	11.73 10.5	[8] [10]	10.5 ± 0.8 (13.8 ± 1.2)	11.3 ± 0.6 (14.4 ± 0.6)
7 OCB	–		10.0 ± 0.4 (12.5 ± 0.5)	9.0 ± 0.4 (11.2 ± 0.5)
8 OCB	12.40 (S_A)	[8]	10 ± 1 (13 ± 1)	11 ± 1 (14 ± 1)
5 CB	10.9 ± 0.1	[38]	11 ± 1 [37]	
6 CB	–		8.1 ± 1 [35] (10.1 ± 1)	
8 CB	10.9 ± 0.1	[38]		
5 PCH	–		17.4 ± 0.3 [24] (19.6 ± 0.3)	
7 PCH	–		14.4 ± 0.5 [24] (18.4 ± 0.5)	

[a] Meier and Saupe formula (3).
[b] Coffey et al. formula (4).

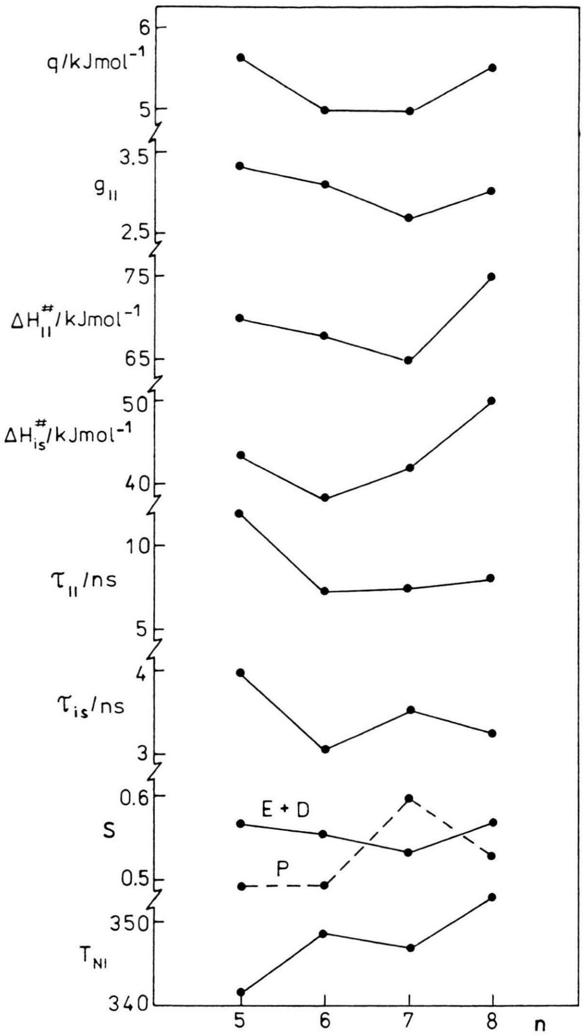

Fig. 8. Dependences of the measured quantities upon the number of carbon atoms in the alkyloxy chains of *n*OCB compounds. S and q are taken at $T_{NI} - T = 10$ K, τ_{is} and $\tau_{\parallel}$ are extrapolated to T_{NI}.

In Fig. 6 we compare the temperature dependencies of the nematic potential and the order parameters obtained according to both normalization procedures. As can be seen, both quantities exhibit a roughly similar behavior within the nematic phase. This seems to justify the next step in evaluation of the results. In Fig. 7 the nematic potentials are plotted versus the order parameter in order to check the relation (2). The values of X_a taken from [8] and [10] are also included in the plots for 6 OCB and 8 OCB. For each substance the points do not lie exactly on the lines going through the origin. This concerns also the NMR results of Dong et al. [10] for 6 OCB. On the other hand, the data of Councell et al. [8] fulfill (2) almost exactly. In the Figs. 6 and 7 we have marked for q-values the error bars arising from the dielectric relaxation studies, but the errors caused by the way of obtaining of the order parameters cannot be easily estimated. There exists a marked difference between the $q(S)$ behaviors obtained by both NMR-groups for 6OCB, although the $q(T)$ dependencies are closer; this suggests that they obtained different order parameters for the same substance using the same experimental method. Especially a proper $S(T)$ dependence in the vicinity of the clearing point is desired.

The slopes of the lines drawn through the experimental points and the origin give the values of the strength coefficient $\mathscr{E}$. They are listed in Table 3 together with the accessible data for other cyano-compounds. Both normalization procedures applied in calculations of the order parameters give different strength parameters. However, the consistency of the NMR and present dielectric results is quite close. So the NMR data can be used as a test of the correctness of (3) and (4). Rather unexpectedly, the old Meier-Saupe formula seems to be better in the case of *n*OCB compounds as well as for some *n*CB substances [35].

To summarize the results, we plotted all obtained quantities as functions of the number of carbon atoms in the alkyloxy chain of *n*OCB compounds in Figure 8. No special odd-even effects can be seen. It may only be noted that all parameters characterizing the molecular dynamics in pentyloxycyanobiphenyl are relatively high in comparison with the next two nematogens in the series. That might indicate stronger intermolecular interactions in this substance.

[1] B. Gestblom and S. Wróbel, Liq. Cryst. **18,** 31 (1995).
[2] D. Demus and H. Zaschke, Flüssige Kristalle in Tabellen, Vol. II, VEB Leipzig 1984.
[3] P. E. Cladis, R. K. Bogardus, W. B. Daniels, and G. N. Taylor, Phys. Rev. Lett **39,** 720 (1977).
[4] S. Chandrasekhar, Liquid Crystals, Cambridge University Press, 2nd ed., Cambridge 1992.
[5] A. Buka, P. G. Owen, and A. H. Price, Mol. Cryst. Liq. Cryst. **51,** 273 (1979).
[6] T. M. Takahashi, S. Mita, and S. Kondo, Mol. Cryst. Liq. Cryst. Letters **3,** 43 (1986).
[7] G. Czechowski, B. Żywucki, and J. Jadżyn, SPIE vol. **1845,** Liq. and Solid State Cryst. (1992), p. 527.
[8] C. J. R. Counsell, J. W. Emsley, G. R. Luckhurst, and H. S. Sachdev, Mol. Phys. **63,** 767 (1988).
[9] J. W. Emsley, G. R. Luckhurst, and H. S. Sachdev, Liq. Cryst. **5,** 953 (1989).
[10] R. Y. Dong and G. Ravindranath, Liq. Cryst. **17,** 47 (1994).
[11] C.-D. Poon, C. M. Wooldridge, and B. M. Fung, Mol. Cryst. Liq. Cryst. **157,** 303 (1988).
[12] W. Maier and A. Saupe, Z. Naturforsch. **13a,** 564 (1958); **14a,** 882 (1959); **15a,** 287 (1960).
[13] G. Meier and A. Saupe, Mol. Cryst. **1,** 515 (1966).
[14] A. J. Martin, G. Meier, and A. Saupe, Symp. Faraday Soc. **5,** 119 (1971).
[15] W. Maier and G. Meier, Z. Naturforsch. **16a,** 262 (1961).
[16] W. T. Coffey and Yu. P. Kalmykov, Liq. Cryst. **14,** 1227 (1993).
[17] W. T. Coffey, D. S. F. Crothers, and J. T. Waldron, Physica A **203,** 600 (1994).
[18] W. T. Coffey, D. S. F. Crothers, Yu. P. Kalmykov, and J. T. Waldron, Physica A **213,** 551 (1995).
[19] W. T. Coffey, Yu. P. Kalmykov, and J. T. Waldron, Liq. Cryst. **18,** 677 (1995).
[20] W. H. de Jeu, Physical Properties of Liquid Crystalline Materials, Gordon and Breach, London 1980.
[21] H. Kresse, Adv. Liq. Cryst. **6,** 109 (1983).
[22] S. Urban, H. G. Kreul, and A. Würflinger, Liq. Cryst. **12,** 921 (1992).
[23] B. Gestblom and S. Urban, Z. Naturforsch. **50a,** 595 (1995).
[24] S. Urban, B. Gestblom, T. Brückert, and A. Würflinger, Z. Naturforsch. **50a,** 984 (1995).
[25] H. G. Kreul, S. Urban, and A. Würflinger, Phys. Rev. A **45,** 8624 (1992).
[26] A. Würflinger, Ber. Bunsenges. Phys. Chem. **95,** 1040 (1991).
[27] V. I. Minkin, D. A. Osipov, and Yu. A. Zhdanov, Dipole Moments in Organic Chemistry, Plenum, New York 1970.
[28] H.-H. Graf, H. Kneppe, and F. Schneider, Mol. Phys. **77,** 521 (1992).
[29] S. Urban, E. Novotna, H. Kresse, and R. Dąbrowski, Mol. Cryst. Liq. Cryst. **262,** 257 (1995).
[30] C. Druon and J. M. Wacrenier, Mol. Cryst. Liq. Cryst. **88,** 99 (1982).
[31] S. Urban, T. Brückert, and A. Würflinger, Z. Naturforsch. **49a,** 552 (1994).
[32] T. Brückert, S. Urban, and A. Würflinger, Ber. Bunsenges. Phys. Chem., in print.
[33] T. Brückert and A. Würflinger, private information.
[34] M. Mitra, S. Paul, and R. Paul, Z. Naturforsch. **46a,** 858 (1991).
[35] S. Urban and A. Würflinger, Adv. Chem. Phys., Vol. **98,** Chapt. 2 (1996).
[36] S. Urban and A. Würflinger, Liq. Crystals **12,** 931 (1992).
[37] S. Urban, H. G. Kreul, and A. Würflinger, Liq. Crystals **12,** 921 (1992).
[38] C. J. R. Counsell, J. W. Emsley, N. J. Heaton, and G. R. Luckhurst, Mol. Phys. **54,** 847 (1985).